Low-cost, simple and eco-friendly biosynthesis of CeO2-NPs using extract of Pelargonium hortorum for the photocatalytic and antioxidant applications

Ali Ganbarianzade Mahabadi
Islamic Azad University
Abbas Mirzakhani
Agricultural Research, Education and Extension Organization (AREEO)
Amir Azizi (a-azizi@araku.ac.ir)
Faculty of Science, Arak University https://orcid.org/0000-0003-2741-6797
Saied Chavoshi
Arak Branch, Islamic Azad University
Shahab Khaghani
Arak Branch, Islamic Azad University

Original Research Full Papers

Keywords: Phytochemical composition, Pelargonium hortorum extracts, Biosynthesis, CeO2 -NPs, Practical application

Posted Date: February 1st, 2021

DOI: https://doi.org/10.21203/rs.3.rs-161201/v1

Low-cost, simple and eco-friendly biosynthesis of CeO_2-NPs using extract of Pelargonium hortorum for the photocatalytic and antioxidant applications

1. A. Ganbarianzade Mahabadi [a],

Address and Affiliation: Department of Horticulture Science, Arak Branch, Islamic Azad University, Arāk, Iran

Email: ganbariyanali@gmail.com

2. A. Mirzakhani [ab],

Address and Affiliation: Horticulture Crops Researcher Department, Markazi Agricultural and Education center, Agricultural Research, Education and Extension Organization (AREEO), Arak, Iran

Email: Mirz51@yahoo.com

3. A. Azizi [c*] (Corresponding Author),

Address and Affiliation: Department of Chemistry, Faculty of Science, Arak University, Arak, Iran
Postal code: 38156-8-8138
Tel.: +98 86 32627536; fax: +98 86 32777400
Email: a-azizi@araku.ac.ir

4. S. Chavoshi [d]

Address and Affiliation: Department of Agronomy and Plant Breeding, Arak Branch, Islamic Azad University, Arāk, Iran

Email: s-chavoshi@iau-arak.ac.ir

5. Sh. Khaghani [d]

Address and Affiliation: Department of Agronomy and Plant Breeding, Arak Branch, Islamic Azad University, Arāk, Iran

Email: shahab.khaghani@gmail.com

Abstract

In this paper, firstly the phytochemical composition in the aqueous extract of *Pelargonium*, growing wildly in the center of Iran, was studied. Folin–Ciocalteu and Aluminum chloride methods and the GC/MS technique were used to determine the total phenolic, flavonoid contents, and volatile constituents in the extract, respectively. The amounts of the total phenolic and flavonoid contents in the extract were found to be 136.5 mg GA/g and 63.9 mg RU/g, respectively. Twenty-one compounds, representing 15 (about 80.0%) of the total volatile constituents were identified. The main components of the volatile constituent were α-pinene (25.28%) and fenchyl acetate (20.63%). Secondly, a fast, simple, and eco-friendly biosynthesis of cerium oxide nanoparticles (CeO_2-NPs) were investigated using the extract of *Pelargonium* as a natural reducing and stabilizing agent. Several advance techniques such as Ultraviolet-Visible (UV–Vis) spectroscopy, X-ray diffraction (XRD), Scanning electron microcopy (FESEM), Dynamic light scattering (DLS), and Brunaure Emmett-Teller (BET) were used for the analysis and characterization of the synthesized nanoparticles. The results of the characterization analysis showed that the prepared nanoparticles were spherical in shape, with an average size of 28 nm and zeta potential of -25.8 mV, and had 33.84 m^2/g BET surface area, 9.31 nm mane diameter pore, and a total pore volume of 0.078 cm^3/g. Finally, the practical applications including the antioxidant and photocatalyst activity of the biosynthesized CeO_2-NPs were evaluated. An analysis of antioxidant and catalytic activities showed that the biosynthesized CeO_2-NPs have a good ability of scavenging of 2,2-diphenyl-1-picrylhydrazyl (DPPH) free radical with the IC_{50} value of 42.7 μg/mL and also good reduction ability of hexavalent chromium {Cr(VI)} ions with a reduction efficiency of 94% in an aqueous solution containing 10 mg/L of Cr(VI) of ion with natural pH of 5.5 and CeO_2-NPs dose of 200 mg/L during 60 min.

Keywords: Phytochemical composition, *Pelargonium hortorum* extracts, Biosynthesis, CeO_2 -NPs, Practical application

1. Introduction

Cerium oxide nanoparticle (CeO_2-NPs) is one of the important metal oxides that could be used in optical, medical, and catalytical applications for its unique physicochemical properties including biocompatibility, high stability, and special surface chemistry [1–3]. CeO_2-NPs are usually synthesized via chemical methods, which mostly employ toxic reducing agents, posing various threats to the environment. In addition, the CeO_2 prepared with these methods is toxic and unstable, reducing its efficiency [4,5]. Accordingly, in recent decades, a safe, non-toxic, eco-friendly, and low cost approach, known as biological (green) synthesis, is used by researchers for production of metal oxide nanoparticales, including CeO_2 [6–8]. This approach employs various biological resources such as plants, microbes, or any other biological derivative (primary and secondary metabolites) believed to lead to reduction and stabilization. Studies show that these compounds are polyphenols, flavonoids, tannic acid, terpenoids, carbohydrates, amines, enzymes, etc., which function as natural antioxidants [1,9]. In general, the high antioxidant activity of the plant or microorganism results in an extract or any other biological derivative with high reducing capacity, which in turn increases the efficiency of the synthesized nanoparticle [9].

Numerous published studies are available on biological synthesis of CeO_2-NPs using plant extracts or other biological derivatives for multipurpose applications. In these studies, green synthesized CeO_2-NPs have been mostly examined for biomedical purposes such as antimicrobial, anticancer, anti-larvicidal, and antioxidant therapies and photocatalytic degradation of organic compound applications [2–11]. However, there are few studies dealing with an antioxidant and the photocatalytic role of CeO_2-NPs synthesized by the green method on heavy metal ions of wastewater treatment. For example, Xiao et al. reported an excellent photocatalytic activity for $CeO_2/BiOIO_3$ heterojunction with oxygen vacancies and Ce^{4+}/Ce^{3+} redox and its application in removal of the Hg^{2+} ion [12]. Balakumar et al. (2019) used an

ultrasound-assisted method to improve the structure of CeO_2@polyprrole core-shell nanosphere and its photocatalytic reduction of Cr(VI) [13]. Kashinath et al reported microwave mediated synthesis and characterization of CeO_2-GO hybrid composite for removal of chromium ions and their antibacterial efficiency [14]. Saravanakumar et al. reported construction of novel Pd/CeO_2/g-C_3N_4 nanocomposites as efficient and visible-light photocatalysts for hexavalent chromium detoxification [15]. In another study, multi-functional properties of ternary CeO_2/SnO_2/rGO nanocomposites, including visible light driven photocatalyst and heavy metal (Cd^{2+} and Pb^{2+}) removal were reported by Priyadharsanet al. [16].

The aim of this research is biological synthesis of CeO_2-NPs using aqueous extracts of *Pelargonium hortorum*, a growing plant in Iran, as a natural reducing and stabilizing agent. *Pelargonium* belongs to the *Geraniaceae* family with about 300 species, mostly known as an ornamental plant; however, it is also used in the manufacture of herbal medicines for its unique medicinal properties [17]. The literature includes studies using several flavonoids in extracts extracted from geranium, including quercetin 3-O-glucoside, quercetin 3-O-pentose, isorhamnetin aglycone, kaempferol 3-O-, kaempferol 3-O-glucoside, kaempferol 3,7-di-O-glucoside, rhamnoside-glucoside, quercetin 3-O-pentoside-glucoside, myrisetin 3-O-glucoside-rhamnoside, and quercetin 3-O-rhamnoside-glucoside [17,18]. These compounds (polyphenolic compounds including flavonoids) act as natural reducing agents in extracts and it is predicted that these extracts could act as a potent green and non-toxic reluctant in synthesis of nanoparticles [9,18]. There is paucity of research on the use of *geranium* extract for synthesis of metal oxides. Most of the studies mentioning the ability of *geranium* extract as a reducing agent reported synthesis of noble metals nanoparticles such as silver and gold and their application in medicine [18–22]. The review of the literature carried out in this study indicated that so far there is no phytochemical study of *Pelargonium hortorum* and its use for

biosynthesis of pure CeO_2-NPs for antioxidant and photocatalytic applications, and especially in the photocatalytic reduction of hexavalent chromium, Cr(VI), ions.

Chromium ion has been classified as an important water pollutant, which mostly appears in form of Cr(VI) and Cr(III) states in aquatic environments. Cr(VI) is widely found in wastewater originating from many industries dependent on chromium; thus, concentration of Cr(VI) in the effluent of these industries is higher than the allowable limit extractable (0.1 mg/L) in surface waters [23–25]. According to the literature, ions of Cr(VI) are more toxic than Cr(III) ions, thus, more dangerous to the environment and health of living organisms; therefore, reduction of Cr(VI) to Cr(III) ions could be a suitable strategy for reducing the risks of Cr(VI) ions and easy separation of this ion from water. Given solubility of Cr(VI) ions in water, it is difficult to remove them from water whereas Cr(III) ions can be easily precipitated by alkalizing the solution and separated in solid sludge form [26,27].

To the best of my knowledge, this study is the first report on chemical composition of the extract of *Pelargonium hortorum*, grown in central Iran, looking for a simple and eco-friendly biosynthesis of pure cerium oxide (CeO_2-NPs) using this extract as a green bioreducing reagent. In this regard, the phytochemical composition including total phenolic, flavonoid, and volatile constituents in the extract of *Pelargonium hortorum* was determined by Folin-Ciocalteu and aluminum chloride methods and GC/MS technique, respectively. In addition, the microstructure, optical properties, and some other properties of the biosynthesized CeO_2-NPs were characterized by using various advanced techniques including Ultraviolet-Visible (UV–Vis) spectroscopy, X-ray diffraction (XRD), Dynamic light scattering (DLS), and Brunaure Emmett-Teller (BET). Moreover, the performance of the biosynthesized nanoparticles was used in 2,2-diphenyl-1-picrylhydrazyl (DPPH) free radical scavenging and photocatalytic reduction of Cr(VI) ions as the model metal ion.

2. Materials and method

2.1. Materials

The *Pelargonium hortorum* plants used for the study were collected from the center of Iran (Arak, Markazi province) at the beginning of Aug 2020 and were used after they were approved by the herbarium expert of the Botanical Garden of Arak University. The materials applied in this study were purchased from Merck and Aldrich chemical companies with high purity and used as such, without further purification. For example, Cerium nitrate purity ≥99.0% was purchased from Aldrich. Potassium dichromate (>99.9%), 1,5-diphenylcarbohydrazide (DPC) purity>99.0%, for metal indication, n-hexane (purity >99%), anhydrous sodium sulfate (>98.5%), hydrochloric acid purity >36%, sodium hydroxide (>97%), methanol (purity >99%), and ethanol with purity of >99.9%, were all Merck products. Folin–Ciocalteu reagent was purchased from Sigma-Aldrich Corporation. Gallic acid (GA) with purity of >98%, sodium carbonate (purity >99%), rutin (RU) with purity of >97%, and aluminum chloride (purity >98.9%) were also purchased from Merck. Double distilled water with conductivity of less than 0.2 μS/cm was used in this study for preparation of all of the experiment solutions.

2.2. Method

2.2.1. Preparation of the *Pelargonium hortorum* extract

For this purpose, first some parts of fresh leaves and flowers of *Pelargonium hortorum* were selected and washed. Then 10 g of this material were carefully weighed and transferred to a 250 mL beker containing 100 mL of double distilled water. The prepared mixture was heated below the boiling temperature for 1 hour. Finally, the prepared solution was cooled and filtered and then stored in a dark bottle at 4 ° C until use in the next steps.

2.2.2. Determination of the phytochemical composition

Total phenolic and flavonoid contents of the *Pelargonium hortorum* aqueous extract after addition of Folin-Ciocalteu and aluminum chloride as the coloring agents were determined by

a UV-Vis spectrophotometer at λ_{max} = 765 nm and λ_{max} = 415 nm, respectively [28,29]. Briefly, 0.5 mL of each diluted extract was mixed with 0.5 mL of each reagent (Folin–Ciocalteu reagent in presence of sodium carbonate or 5% aluminum chloride methanolic solution). After 30 min, the absorbance rates were read at 765 nm and 415 nm, respectively, for determining the total phenolic and favonoid contents. To determine the total phenolic and flavonoid contents by standard calibration curves of gallic acid (GA) and rutin (RU) was used and the results were expressed as milligrams of GA and RU equivalent per gram of each extract (mg GA/g and mg RU/g) [28, 29].

The volatile compounds in the *Pelargonium hortorum* aqueous extracts were isolated using Syringe to Syringe dispersive liquid–phase microextraction (SS-DLPME) method [30]. N-hexane was applied as the extraction solvent. Briefly, 2 mL of aqueous extract were put in a Syringe and then mixed with 2 mL n-hexane solvent. After agitation for 10 min, 2 mL of the organic solvent was separated by decantation, dried with anhydrous sodium sulfate, and then concentrated to 1 mL by evaporation under vacuum at 50°C. Finally, the concentrated product was injected into the chromatograph coupled with mass detector {GC/MS (GC: HP 6890, MS: HP 5973), column (HP5-MS, 30 m×0.25 mm fused silica capillary column)} to determine the volatile compounds.

2.2.3. Biosynthesis of CeO_2-NP

The biological synthesis of CeO_2-NP was performed according to the common methods reported in the literature [6–8] yet with some modifications and optimization in the synthesis effectiveness variable, including the cerium salt concentration, extract volume, temperature, and time. Optimizations in the process of synthesizing CeO_2-NP was based on achieving the highest absorption spectra intensity within 300–330 nm (due to charge transfer from O_{2P} to Ce_{4f} orbitals) [31], which was measured and recorded by a UV-Vis spectrophotometer. Under optimum condition, 20 mL of aqueous extract of *Pelargonium hortorum*, as the reducing agent,

was added to 80 mL of 0.1 M cerium solution (2.91 g of $Ce(NO_3)_2.6H_2O$ salt were dissolved in 100 mL double distilled water). Then the solution was mixed by magnetic stirring for 2h at 80°C and the water was removed until a whitish-brown gel was obtained, which indicated the biosynthesis of cerium nanoparticale compounds [32]. The obtained gel was washed several times with double distilled water and ethanol and then was air dried in an oven at 70 °C for 1 h. Finally, the dried biosynthesized produced was calcined at 400 C for 2 h.

2.3. CeO_2-NPs characterization

A UV-Vis spectrophotometer (dynamic HaloXB-10) was used to confirm the successful formation of CeO_2-NPs during the biosynthesis method and also to determine the optical properties of the CeO_2-NPs. Fourier-transform infrared spectroscopy (FTIR Bruker alpha Pusing the KBr pellets) was used to determine the functional groups present in the synthesized CeO_2-NPs within the range of 4000–400 cm^{-1}. In order to determine the phase and the crystal structure of the synthesized CeO_2-NPs, a separate XRD (ITAL-Structures-APD 2000) with Cu Ka radiation X-ray source was used. To analyze the distribution size and zeta potential of CeO_2-NPs, a DLS analyzer (HORIBA SZ-100) was applied. Field emission scanning electron microscopy (FESEM, TESCAN, and Mira III) was employed to determine the morphology of CeO_2-NPs. The EBT N_2-adsorption (BELSORP, Mini II) was carried out to determine the surface properties of the biosynthesized CeO_2-NPs.

2.2.4. Antioxidant activity

The free radical scavenging activity of the *Pelargonium hortorum* aqueous extract and the biosynthesized CeO_2-NPs was determined by the percentage of 2,2-diphenyl-1-picrylhydrazyl (DPPH) free radical scavenging efficiency [33]. Briefly, 2 mL of either of the *Pelargonium hortorum* aqueous extract or CeO_2-NPs solution in different concentrations (5-100 µg/mL in methanol) was added to 3 mL of methanolic DPPH solution, kept for 30 min in dark, and then

centrifuged. After that, the absorbance of the supernatant at 517 nm was determined using a UV-Vis spectrophotometer. The absorbance at 517 nm of methanolic DPPH solution without aqueous extract or CeO_2-NPs was also analyzed for control. Percentages of radical scavenging (% SCV) were calculated as $\%SCV = \frac{A_0 - A_S}{A_0} \times 100$

(1)

where A_0 is the DPPH control absorbance and A_S is the DPPH absorbance with aqueous extract or CeO_2-NPs.

2.4. Photocatalytic activity

The photocatalytic reduction of the hexavalent chromium ions from aqueous solutions was studied to investigate the photocatalytic activity of the biosynthesized CeO_2-NPs. 10 mg/L of the Cr(VI) ions solution with natural pH of 5.5 was used as a model pollutant to determine the photocatalytic activity. 200 mg of CeO_2-NPs as the photocatalyst was applied for reduction of 1.5 liters solution. A 250 W mercury lamp with the maximum emission at wavelength of 365 nm (inside quartzes tube) placed in the center of a double-walled glass photo-reactor with 2 L capacity was used for the reduction process. The content of the reactor was stirred by a mechanical stirrer and its temperature was controlled by passing water through the outer jacket of the reactor. A UV light source was turned on after 30 min of stirring the solution (in order to evaluate the effect of surface absorption, the solution was stirred for 30 min in darkness). Sampling was done every 10 min. After centrifuging and photocatalyst separation, the residual concentration of Cr(VI) ions was analyzed with the appropriate calibration data by colorimetry method with 1,5-diphenyl carbazide (DPC) in acidic solution at λ max = 542 nm using UV-Vis spectrophotometer [34]. Then the reduction efficiency (*RE*) was calculated by the following equation:

$$\%RE = \frac{[C]_0 - [C]_t}{[C]_0} \times 100 \quad (2)$$

where $[C]_0$ and $[C]_t$ are initial and appropriate time concentrations of Cr(VI) ions, respectively.

3. Results and discussion

3.1. Total phenolic and flavonoid content

Assessment of the results of the study regarding the presence of polyphenolic compounds in the *Pelargonium hortorum* extract, including polyphenols and flavonoids compounds, which were performed by Folin-Ciocalteu and ammonium chloride methods, respectively, showed that the amounts of polyphenols and flavonoids compounds in the extract are 136.5 mg of GA/g extract and 63.9 mg of RU/g extract, respectively. Studies in the literature have reported that presence of polyphenolic compounds in derivatives extracted from microorganisms can act as a non-toxic and natural reagent for fast and eco-friendly biosynthesis of metal nanoparticles and their oxides [9,18]

3.2. Determination of volatile compounds

The volatile compounds in the *Pelargonium hortorum* aqueous extract were prepared using the liquid-liquid extraction by n-hexane solution through SS-DLPME method. The number of volatile components of the organic extract was identified by the GC/MS method. The constituents were identified by comparing their MS spectra with certified reference compounds, and were confirmed by comparison of their retention indices with those of certified reference compounds [35–37]. 17 out of 22 components were detected in the organic extract, which formed about 93.5% of the total extract (Table 1). The major compounds were α-pinene (19.46%), α-fenchyl acetate (16.57%), limonene (11.45%), trans-β-caryophyllene (11.28%) and camphene (8.38%). The analysis of the volatile compounds showed that the identified chemical compounds were much similar to the volatile compounds detected from the specie

grown wildly in the west of Iran [37].

"Table 1"

3.3. Biosynthesized CeO_2-NPs characterization

UV–Visible spectroscopy technique was used for monitoring the formation of CeO_2-NPs. In this technique, successful biosynthesis of CeO_2-NPs was confirmed with respect to the color change of the cerium salt solution from light yellow to whitish-brown after the addition of the drops of the plant extract [32]. In addition, creation of a strong absorption spectra at a maximum wavelength of 325 nm due to surface plasmon resulting to the charge transfer from O_{2P} to Ce_{4f} orbitals was another sign of the production of CeO_2-NPs (Fig 1), which is highly consistent with the reported results [6,31,32]. Also, the optimization of the conditions for the production of the largest amount of CeO_2-NPs with dimensions less than 50 nm was performed by measuring the intensity of the absorption spectra and displacement at the maximum wavelength position by a UV-Vis spectrophotometer. The conditions that lead to recording the highest absorption and displacement spectra of blue shift due to the production of more nanoparticles and their smaller size, respectively, were selected as the optimal conditions. Accordingly, 80 mL of cerium salt of 0.1 M, 20 mL of the extract, temperature 80 °C, and time of 2 h were selected as the optimal conditions for biosynthesis of CeO_2-NPs. Furthermore, the direct optical band gap energy as a property in the biosynthesized CeO_2-NPs was estimated as 3.81 eV by the Tauc equation ($Eg = 1239.8/\lambda$) [38], where Eg and λ are the band gap energy (eV) and wavelength (nm) of the absorption edge in the UV-Vis spectrum, respectively. It should be noted that when the amount of the extract was increased to more than 20 ml, the size of the particle produced was larger (it showed a red shift) and the band gap decreased, a trend that has been reported in some previous studies as well [6]. **"Fig. 1"**

The FT-IR spectroscopy was carried out to identify the functional groups of the biosynthesized CeO_2-NPs. Fig. 2 shows the FT-IR spectrum of the biosynthesized CeO_2-NPs where the broad

peak was located at 3450 cm^{-1} of the attributed O-H stretching, which might be because of the presence of water. Other strong bands were 1050 and 486 cm^{-1}, which can be attributed to the stretching of the ending vibrations of the O-Ce-O and, Ce-O respectively [39]. The results of this analysis showed that there was no functional group of the extract on the biosynthesized CeO_2-NPs due to calcination at 400 °C. " **"Fig. 2"**

Fig. 3 displays the XRD pattern of the biosynthesized CeO_2-NPs. As shown in this pattern, the peaks that appear at 2θ = 27.78°, 32.20°, 46.16°, 54.46°, 58.55°, 69.12°, and 77.56° are indexed to (111), (200), (220), (311), (222), (400), and (420) facets, respectively. These peaks corresponded to the high purity single phase of CeO_2-NPs and in a face center of the fluorite cubic structure according to JCPDS No. 34-03942, which is in good agreement with the reported results in the previous studies [6,40]. The crystalline size of the biosynthesized CeO_2-NPs was calculated using Scherrer's formula ($D=0.89\lambda/\beta cos\theta$) [41] and was accordingly found to be 29 nm for the highest peak at 2θ=25.22°. **"Fig. 3"**

Moreover, a DLS analysis was applied to determine the zeta potential charge (ZPC) and estimate the hydrodynamic particle size distribution of the biosynthesized CeO_2-NPs, as shown in Fig. 4. It was found that the net surface charge of the biosynthesized CeO_2-NPs was –25.8 mV, which shows its good colloidal stability [6]. Also, the DLS histogram (inset in Fig.4) indicates that the biosynthesized CeO_2-NPs has a narrow pattern with an average hydrodynamic diameter of about 34 nm.

Furthermore, FE-SEM image was used to identify the morphology and estimate the particle size of the biosynthesized CeO_2-NPs (see Fig. 5). This figure shows a uniform distribution of the biosynthesized CeO_2-NPs and a spherical shape as well as a mean particle size of 33 nm, which is in good agreement with the estimated results from the XRD and DLS techniques. In addition, the EDX analysis (illustrated in Fig. 5) was used to study the chemical elements in the biosynthesized CeO_2-NPs. The EDX results showed the major peaks correspond to the Ce

and O element. Such correspondence was not detected for other elements, which confirms the purity of the biosynthesized CeO_2 -NPs. **"Figs.4 & 5"**

Also, the specific surface area, pore volume, and pore radius of the biosynthesized CeO_2-NPs were characterized by N_2 adsorption–desorption porosimetry using a BET analyzer. Fig 6 shows the N_2 adsorption-desorption isotherm of the biosynthesized CeO_2-NPs. This isotherm exhibits a type IV isotherm with an H_2 hysteresis loop in the p/p_0 range of 0.35-0.98, which indicates formation of a mesoporous host in all the CeO_2-NP structures [42]. The BET-specific surface areas of the biosynthesized CeO_2-NPs are 33.84 m^2/g with mean pore diameters of 9.31 nm and total pore volume of 0.078 cm^3/g. The inset figure shows the pore size distribution of CeO_2-NPs. The main peak was located in the range of about 2.4 nm, which confirms the mesoporous nanoparticles classification [42]. **"Fig. 6"**

3.4. Antioxidant activity

The antioxidant potential of the *Pelargonium hortorum* extract was evaluated by the scavenging potential of stable methanolic DPPH free radicals (Fig. 7). In the presence of the extract, the color of the DPPH solution changed from deep violet to light yellowish with an increase in the contact time [33]. The percentage of the scavenging of DPPH increased with an increase in the extract amount from 5 to 100 µg/mL and reached about 85.4% at about 100 µg/mL. The results suggest that the phenolic components (total phenol and flavonoid) contributed significantly to the antioxidant capacity of the extract. The antioxidant activity of the biosynthesized CeO_2-NPs was also evaluated using the DPPH method. The maximum antioxidant activities (69.8%) were exhibited when 100 µg/mL of the CeO_2-NPs was used. Since 100% of the free radical could not be scavenged by a certain substance [43], the antioxidant potential was evaluated by the IC_{50} value (the scavenging concentration needed to scavenge 50% of the DPPH free radical) of the substance. The results show that the IC_{50} of

extract and CeO_2-NPs were found to be 29.3 µg/mL and 42.7 µg/mL, respectively.

"Fig. 7"

3.5. Photocatalytic activity

The photocatalytic activity of the biosynthesized CeO_2-NPs was studied by determining the reduction of 1.5 L of Cr(VI) ions in an aqueous solution (10 mg/L) with a natural pH of 5.5 under irradiation with UV light using 200 mg/L CeO_2-NPs as the photocatalyst. About 94% Cr(VI) ions reduction was achieved after 60 min treatments. The photocatalytic reaction mechanism of the biosynthesized CeO_2-NPs is suggested when CeO_2-NPs are excited by light, as a result of which the electrons (e^-) from the valence band move to the conduction band leaving a hole (h^+) in the valance band [6]. The formation of the electrons in the conduction band plays a role in the reduction of the Cr(VI) ions. The reaction mechanism in equations (3-6) is a follows:

$$CeO_2 + hv \rightarrow CeO_2(e^- + h^+) \quad (3)$$

$$3CeO_2(e^- + h^+) + 3Cr(VI) \rightarrow Cr(III) + 3CeO_2(h^+) \quad (4)$$

$$3CeO_2(h^+) + 3H_2O \rightarrow 6HO^\bullet + 3CeO_2 \quad (5)$$

$$6HO^\bullet \rightarrow 3H_2O_2 \quad (6)$$

which, in acidic media indirectly was generated H_2O_2 molecules leads to rapid reduction of Cr(VI)ions [44]. In this section, the kinetic reduction of the Cr(VI) ions was also investigated and analyzed by $-ln\frac{C_0}{C_t} = kt$ equation. From the slope of $ln\frac{C_0}{C_t}$ plot versus time (Fig. 8), the rate constant (k) was obtained as 0.079 1/min and the coefficient (R^2) was also determined as 0.981 for the process. The rate of the Cr(VI) ions reduction in this process was fitted to the pseudo-first-order kinetic model. Finally, the stability of the biosynthesized CeO_2-NPs was evaluated after its regeneration. Briefly, the used CeO_2-NPs was washed with hydrochloric acid 0.1 M and then sonicated in boiling double distillate water for 15 min, and then dried in oven

at 80 °C for 2 h. The results revealed (Fig. 8) that the Cr(VI) reduction efficiency after a six time treatment process was reduced about 6%. "**Fig. 8"**

Conclusions

In this work, the phytochemical composition in the aqueous extract of *Pelargonium hortorum* from Iran, was studied. The amounts of the total phenolic and flavonoid contents in the extract were found to be 136.5 mg GA/g and 63.9 mg RU/g, respectively. Seventeen compounds (about 93.5%) of the total volatile constituents were identified. α-pinene (25.28%) and fenchyl acetate (20.63%) were the main components of the volatile constituent. The aqueous extract of *Pelargonium hortorum* was used to eco-friendly biosynthesis of CeO_2-NPs. Different techniques were used for the characterization of biosynthesized CeO_2-NPs. The prepared CeO_2-NPs were spherical in shape, with an average size of 28 nm. The synthesized CeO_2-NPs had 33.84 m^2/g BET surface area, 9.31 nm mane diameter pore, and a total pore volume of 0.078 cm^3/g. The IC_{50} value of 42.7 µg/mL was determined for biosynthesized CeO_2-NPs. The reduction efficiency of 94% in an aqueous solution containing 10 mg/L of Cr(VI) with pH of 5.5 by using 200 mg/L CeO_2-NPs during 60 min was achieved. The rate of the Cr(VI) ions reduction process was fitted to the pseudo-first-order kinetic model with a rate constant of 0.079 1/min.

Acknowledgement

The authors wish to acknowledge the university authorities for providing the financial support to carry out this work.

Disclosure statement

There is no conflict of interest on this research.

References

[1] Nadeem M., Khan R., Afridi K., Nadhman A., Ullah S., Faisal S., Mabood Z. U., Hano C., Abbasi B. H., Green synthesis of cerium oxide nanoparticles (CeO_2 NPs) and their antimicrobial applications: A Review, International Journal of Nanomedicine, 2020, 15:5951-5961.

[2] Das S., Dowding J. M., Klump K. E., McGinnis J. F., Self W. T., Seal S., Cerium oxide nanoparticles: applications and prospects in nanomedicine, Nanomedicine, 2013, 8(9):1483-1508.

[3] Walkey C., Das S., Seal S., Erlichman J., Heckman K., Ghibelli L., Traversa E., McGinnis J. F., Self W. T., Catalytic properties and biomedical applications of cerium oxide nanoparticles, Environmental Science: Nano, 2015, 2(1):33-53.

[4] Rajeshkumar S., Naik P., Synthesis and biomedical applications of cerium oxide nanoparticles–a review, Biotechnology Reports, 2018, 17:1-5.

[5] Magudieshwaran R., Ishii J., Raja K. C. N., Terashima C., Venkatachalam R., Fujishima A., Pitchaimuthu S., Green and chemical synthesized CeO_2 nanoparticles for photocatalytic indoor air pollutant degradation, Materials Letters, 2019, 239:40-44.

[6] Elahi B., Mirzaee M., Darroudi M., Kazemi Oskuee R., Sadri K., Amiri M. S., Preparation of cerium oxide nanoparticles in salvia macrosiphon boiss seeds extract and investigation of their Photo-catalytic activities, Ceramics International, 2018, 45:4790-4797.

[7] Arunachalam T, Karpagasundaram M, Rajarathinam N. Ultrasound assisted green synthesis of cerium oxide nanoparticles using prosopis juliflora leaf extract and their structural, optical and antibacterial properties, Materials Science-Poland, 2017, 35(4):791-798.

[8] Singh K. R. B., Nayak V., Sarkar T., Singh R. P., Cerium oxide nanoparticles: properties, biosynthesis and biomedical application, RSC Advances, 2020, 10(45):27194-27214.

[9] Ebrahiminezhad A., Zare-Hoseinabadi A., Sarmah A. K., Taghizadeh S., Ghasemi Y., Berenjian A., Plant-mediated synthesis and applications of iron nanoparticles, Molecular Biotechnology, 2018, 60:154-168.

[10] Maqbool Q., Nazar M., Naz S., Hussain T., Jabeen N., Kausar R., Anwaar S., Abbas F., Jan T., Antimicrobial potential of green synthesized CeO_2 nanoparticles from olea europaea leaf extract, International Journal of Nanomedicine, 2016, 11:5015-5025.

[11] Miri A, Darroudi M, Sarani M. Biosynthesis of cerium oxide nanoparticles and its cytotoxicity survey against colon cancer cell line, Applied Organometallic Chemistry, 2020, 24(1):e5308.

[12] Xiao Y., Tan S., Wang D., Wua J., Jia T., Liu Q., Qi Y., Qi X., He P., Zhou M., $CeO_2/BiOIO_3$ heterojunction with oxygen vacancies and Ce^{4+}/Ce^{3+} redox centers

synergistically enhanced photocatalytic removal heavy metal, Applied Surface Science, 2020, 530:147116.

[13] Balakumar V., Kim H., Manivannan R., Kim H., Ryu J. W., Heo G., Son Y. A., Ultrasound-assisted method to improve the structure of CeO_2@ polyprrole core-shell nanosphere and its photocatalytic reduction of hazardous Cr^{6+}, Ultrasonics Sonochemistry, 2019, 59:104738.

[14] Kashinath L., Namratha K., Byrappa K., Microwave mediated synthesis and characterization of CeO_2-GO hybrid composite for removal of chromium ions and its antibacterial efficiency, Journal of Environmental Sciences, 2019, 76:65-79.

[15] Saravanakumar K., Karthik R., Chen S. M., Vinoth Kumar J., Prakash K., Muthuraj V., Construction of novel Pd/CeO_2/g-C_3N_4 nanocomposites as efficient visible-light photocatalysts for hexavalent chromium detoxification, Journal of colloid and Interface Science, 2017, 504:514-526.

[16] Priyadharsan A., Vasanthakumar V., Karthikeyan S., Raj V., Shanavas S., Anbarasan P. M., Multi-functional properties of ternary CeO_2/SnO_2/rGO nanocomposites: Visible light driven photocatalyst and heavy metal removal Author links open overlay panel, Journal of Photochemistry and Photobiology A: Chemistry, 2017, 346:32-45.

[17] Boukhris M., Simmonds M. S., Sayadi S., Bouaziz M., Chemical composition and biological activities of polar extracts and essential oil of rose-scented geranium, Pelargonium graveolens, Phytotherapy Research, 2013, 27(8):1206-1213.

[18] Mohammadlou M., Jafarizadeh-Malmiri H., Maghsoudi H., Hydrothermal green synthesis of silver nanoparticles using Pelargonium/Geranium leaf extract and evaluation of their antifungal activity, Green Processing and Synthesis, 2017, 6:31-42.

[19] Rivera-Rangel R. D., González-Muñoz M. P., Avila-Rodriguez M., Razo-Lazcano T. A., Solans C., Green synthesis of silver nanoparticles in oil-in-water microemulsion and nano-emulsion using geranium leaf aqueous extract as a reducing agent, Colloids and Surfaces A: Physicochemical and Engineering Aspects, 2018, 536:60-67.

[20] Jafarizad A., Safaee K., Gharibian S., Omidi Y., Ekinci D., Biosynthesis and in-vitro study of gold nanoparticles using Mentha and Pelargonium extracts, Procedia Materials Science, 2015, 11:224-230.

[21] Mirończyk A., Timoszyk A., Koziol J. J., Green synthesis and characterization of gold nanoparticles using Pelargonium zonale extract, Jökull Journal, 2015, 65:300-309.

[22] Franco-Romano M., Gil M. L. A., Palacios-Santander J. M., Delgado-Jaén J. J., Naranjo-Rodríguez I., Hidalgo-Hidalgo De Cisneros J. L., Cubillana-Aguilera L. M., Sonosynthesis of gold nanoparticles from a geranium leaf extract, Ultrasonics Sonochemistry, 2014, 21:1570-1577.

[23] Zhang Y. C., Yang M., Zhang G., Dionysiou D. D., HNO_3-involved one-step low temperature solvothermal synthesis of N-doped TiO_2 nanocrystals for efficient photocatalytic reduction of Cr(VI) in water, Applied Catalysis B: Environmental, 2013, 142–143:249-258.

[24] Norouzi Esfahani R., Khaghani Sh., Azizi A., Mortazaeinezhad F., Gomarian M., Facile and eco-friendly synthesis of TiO_2 NPs using extracts of Verbascum thapsus plant: an efficient photocatalyst for reduction of Cr(VI) ions in the aqueous solution, Journal of the Iranian Chemical Society, 2020, 17:205-213.

[25] WHO, Guidelines for Drinking Water Quality (World Health Organization, Geneva, 2006).

[26] Shirzad Siboni M., Samadi M. T., Yang J. K., Lee S. M., Photocatalytic removal of Cr(VI) and Ni(II) by UV/TiO_2: kinetic study, Desalination Water Treat, 2012, 40:77-83.

[27] Chen D., Ray A. K., Removal of toxic metal ions from wastewaters by semiconductor photocatalysis, Chemical Engineering Science, 2001, 56:1561-1570.

[28] Shaver L. A., Leung S. H., Puderbaugh A., Angel S. A., Two methods of determining total phenolic content of foods and juices in a general, organic, and biological (GOB) chemistry lab, Journal of Chemical Education, 2011, 88:492-495.

[29] Singleton V. L., Orthofer R., Lamuela-Raventós R. M., Analysis of total phenols and other oxidation substrates and antioxidants by means of Folin-Ciocalteu reagent, Methods in Enzymology, 1999, 299:152-178.

[30] Koosha E., Ramezani M., Niazi Ali, Syringe-to-syringe-dispersive liquid–phase microextraction combined with flame atomic absorption spectrometry for pre-concentration and determination of cobalt with the aid of experimental design, International Journal of Environmental Analytical Chemistry, 2018, 98(6):506-519.

[31] Mansingh S., Kandi D., Kumar Das K., Parida K., A mechanistic approach on oxygen vacancy-engineered CeO_2 nanosheets concocts over an oyster shell manifesting robust photocatalytic activity toward water oxidation, ACS Omega, 2020, 5(17):9789-9805.

[32] Muthuvel A., Jothibas M., Mohana V., Manoharan C., Green synthesis of cerium oxide nanoparticles using Calotropis procera flower extract and their photocatalytic degradation and antibacterial activity, Inorganic Chemistry Communications, 2020, 119:108086.

[33] Hung D., Ou, B., Prior, R. L., The chemistry behind antioxidant capacity assays, Journal of Agricultural and Food Chemistry, 2005, 53:1841-1856.

[34] Clesceri L. S., Greenberg A. E., Eaton A. D., Standard methods for the examination of water and wastewater (American Public Health Association, Washington, 1998).

[35] Adams R. P., Identification of essential oil components by gas chromatography/mass spectroscopy, (Allured Publishing Corporation, Illinois, 1995).

[36] Aldermaston, Eight pick index of mass spectra, 2nd Edn, Mass spectroscopy data center, reading, UK 1974.

[37] Taherpour A., Maroofi H., Kheradmand K., Chemical composition of the essential oil of Pelargonium quercetorum Agnew. of Iran, Natural Product Research, 2007, 21(1):24-27.

[38] Tauc J. C., The optical properties of solids (North Holland, Amsterdam, 1972).

[39] Sreekanth T. V. M., Dillip G. R., Lee Y. R, Picrasma quassioides mediated cerium oxide nanostructures and their post-annealing treatment on the microstructural, morphological and enhanced catalytic performance, Ceramics International, 2016, 42(6):6610-6618.

[40] Maqbool Q., Green-synthesised cerium oxide nanostructures (CeO_2-NS) show excellent biocompatibility for phyto-cultures as compared to silver nanostructures (Ag-NS), RSC Advance, 2017, 7:56575-56585.

[41] Hargreaves J. S. J., Some considerations related to the use of the Scherrer equation in powder X-ray diffraction as applied to heterogeneous catalysts, Catalysis, Structure & Reactivity, 2016, 2:33-37.

[42] Sing K. S. W., Williams R. T., Physisorption Hysteresis Loops and the Characterization of Nanoporous Materials, Adsorption Science & Technology, 2004, 22(10):773-782.

[43] Brand-Williams W., Cuvelier M. E., Berset C., Use of a free radical method to evaluate antioxidant activity, Food Science and Technology, 1995, 28:25-30.

[44] Pettine M., Campanella L., Millero F. J., Reduction of hexavalent chromium by H_2O_2 in acidic solutions, Environmental Science and Technology, 2002, 36:901-907.

Table 1 Chemical compositions of the extract from *Pelargonium*.

No.	Components	Retention indices	Retention time (min)	Percentage
1	α-Thujene	922	5.37	0.58
2	α-Pinene	929	5.43	19.46
3	Camphene	941	5.93	8.38
4	β-Pinene	975	6.51	2.89
5	Myrcene	989	6.83	2.45
6	α-Terpinene	1018	7.24	0.81
7	p-Cymene	1021	7.42	1.68
8	Limonene	1027	7.67	11.45
9	ɣ-Terpinene	1055	8.74	1.01
10	α-Terpineol	1085	8.91	0.68
11	Camphor	1145	10.1	2.24
12	α-Fenchyl acetate	1201	12.36	16.57
13	Thymol	1282	13.98	3.63
14	Bornyl acetate	1288	14.27	1.95
15	Trans-β-Caryophyllene	1315	14.75	11.28
16	Germacrene-D	1355	15.76	3.54
17	δ-Cadinene	1381	16.21	4.95
18	Unknown	1427	17.56	1.62
19	Unknown	1452	17.63	1.44
20	Unknown	1508	17.84	0.89
21	Unknown	1582	17.95	1.64
22	Unknown	1591	18.12	0.86

Figure captions

Fig. 1 The UV-Vis spectrum of the biosynthesized CeO_2-NPs

Fig. 2 The FT-IR spectrum of the biosynthesized CeO_2-NPs

Fig. 3 XRD patterns of the biosynthesized of CeO_2-NPs

Fig. 4 Zeta potential charge (ZPC) and the hydrodynamic particle size distribution (inset figure) of the biosynthesized CeO_2-NPs

Fig. 5 The FE-SEM image and EDX spectrum (inset figure) of biosynthesized of CeO_2-NPs.

Fig. 6 N_2 adsorption-desorption isotherm of the biosynthesized CeO_2-NPs. The inset figure is the pore radius distribution of CeO_2-NPs

Fig.7 A comparison the antioxidant potential of the *Pelargonium* extract and biosynthesized CeO_2-NPs

Fig. 8 The kinetic plot in photocatalytic reduction of Cr(VI) ions under: [Cr(VI)]= 10 mg/L, [CeO_2-NPs]= 200 mg/L, pH = 5.5 and t= 60 min. The inset figure is the reuse time results of biosynthesized CeO_2-NPs catalyst

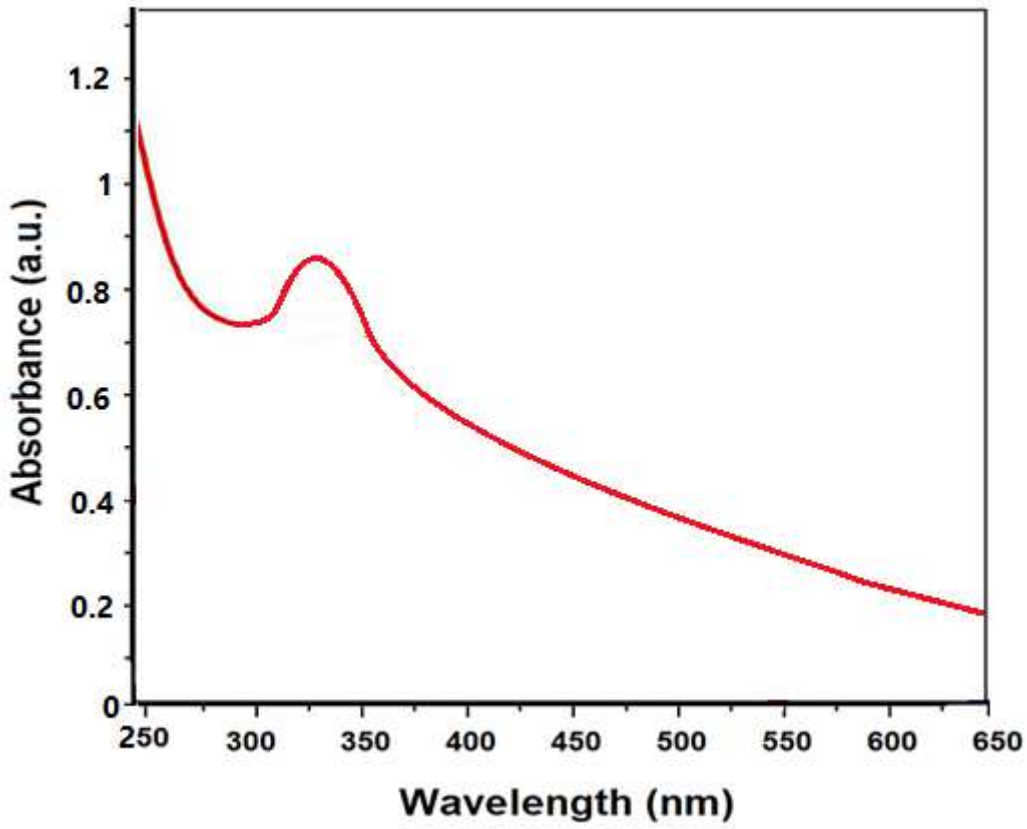
Absorbance (a.u.)
1.2
1
0.8
0.6
0.4
0.2
0
250
300
350
400
450
500
550
600
650
Wavelength (nm)

Fig. 1

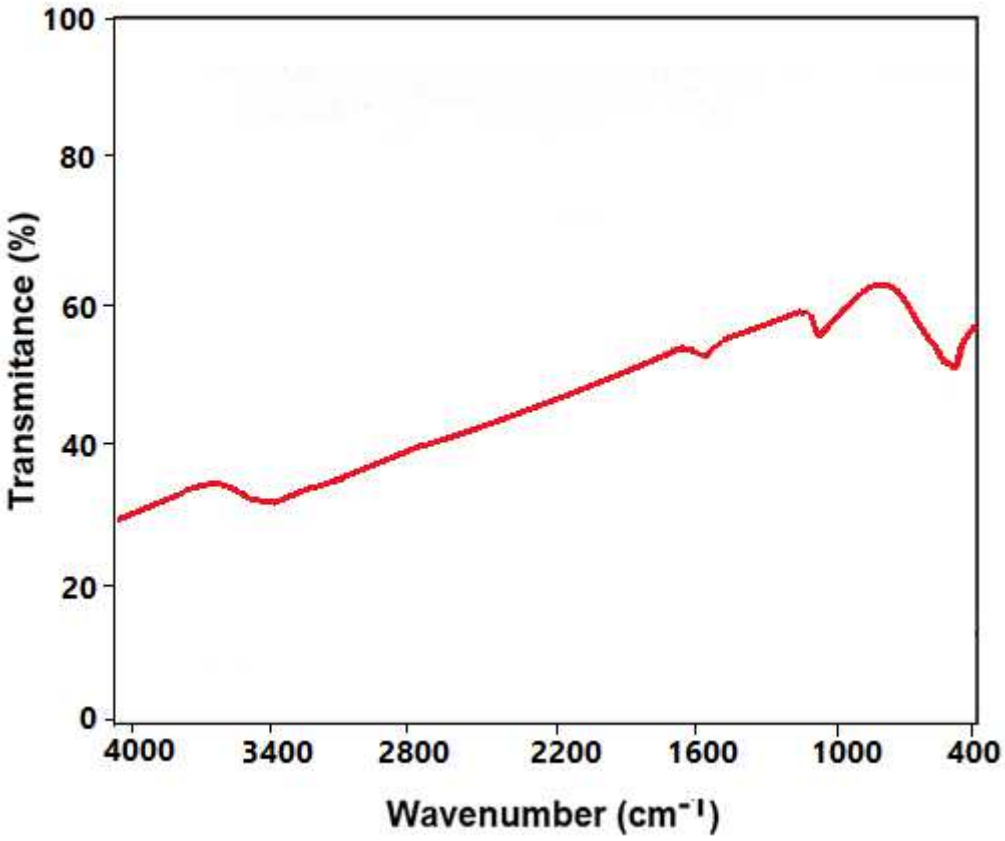
100
80
60
40
20
0
Transmitance (%)
4000
3400
2800
2200
1600
1000
400
Wavenumber (cm⁻¹)

Fig. 2

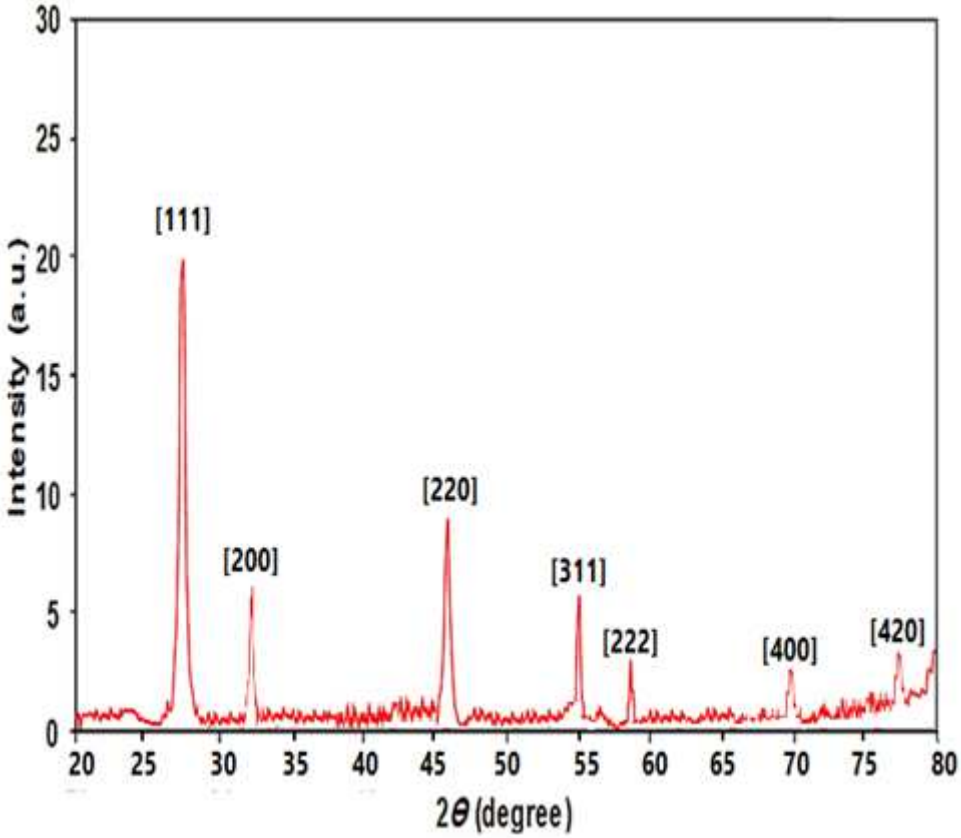
Intensity (a.u.)
2θ (degree)
[111]
[200]
[220]
[311]
[222]
[400]
[420]
0
5
10
15
20
25
30
20
25
30
35
40
45
50
55
60
65
70
75
80

Fig. 3

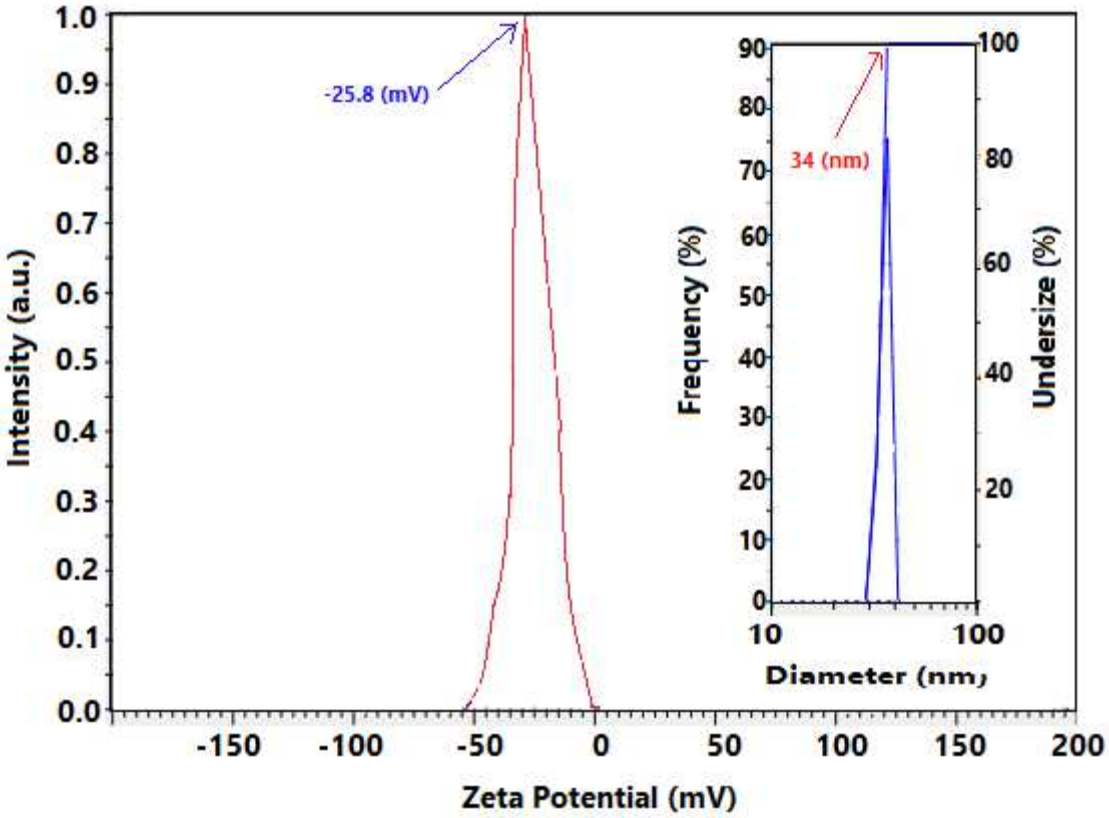
-25.8 (mV)
34 (nm)
Intensity (a.u.)
Zeta Potential (mV)
Frequency (%)
Undersize (%)
Diameter (nm)

Fig. 4

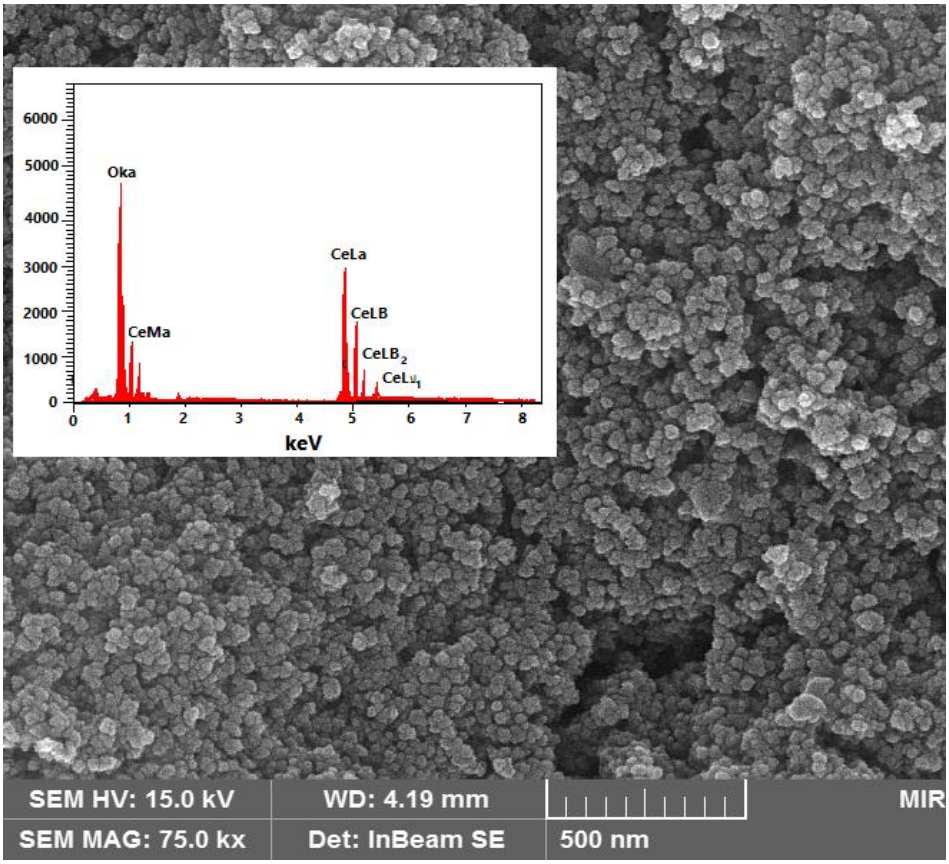
6000
5000
4000
3000
2000
1000
0
Oka
CeMa
CeLa
CeLB
CeLB2
CeLu1
0
1
2
3
4
5
6
7
8
keV
SEM HV: 15.0 kV
WD: 4.19 mm
MIR
SEM MAG: 75.0 kx
Det: InBeam SE
500 nm

Fig. 5

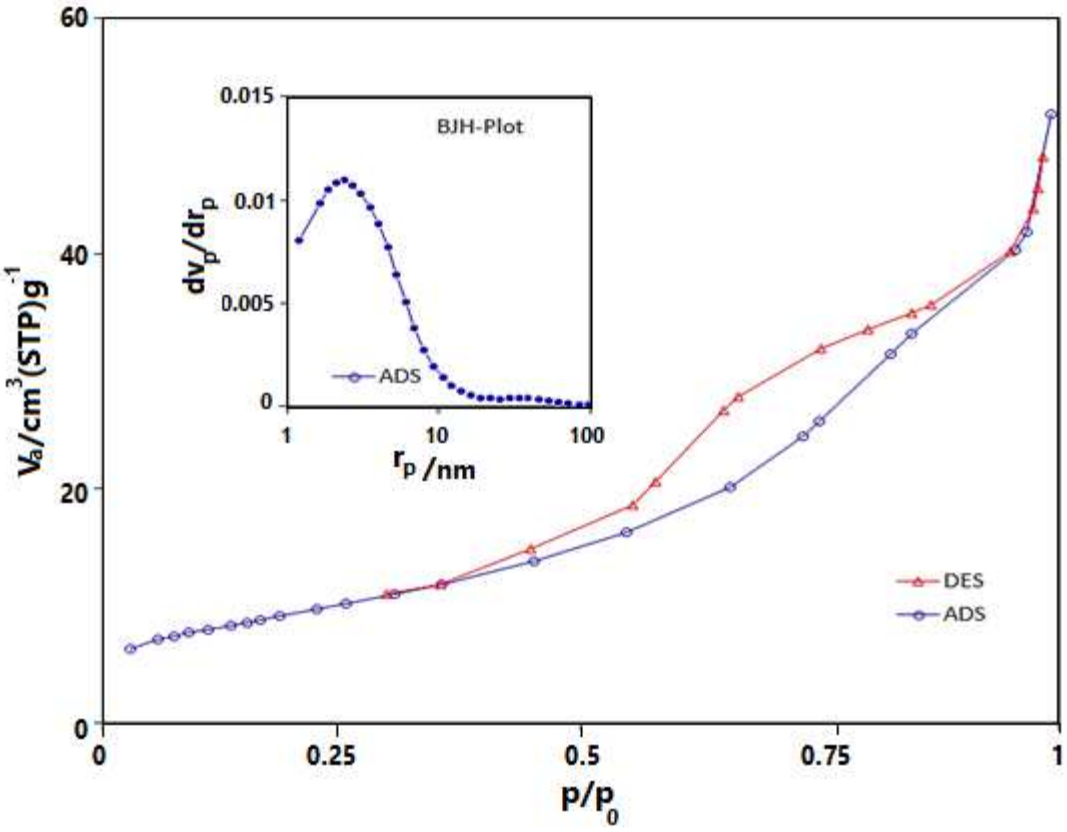
60
40
20
0
0
0.25
0.5
0.75
1
p/p0
Va/cm3(STP)g-1
DES
ADS
BJH-Plot
0.015
0.01
0.005
0
dvp/drp
ADS
1
10
100
rp /nm

Fig. 6

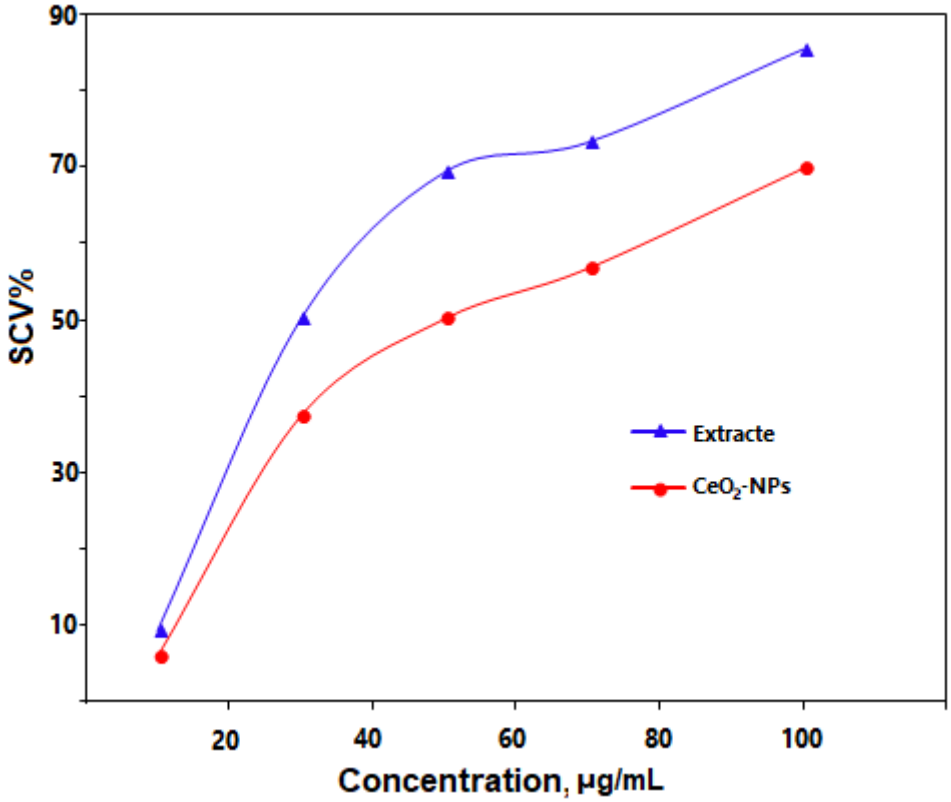
90
70
50
30
10
SCV%
20
40
60
80
100
Concentration, µg/mL
Extracte
CeO2-NPs

Fig. 7

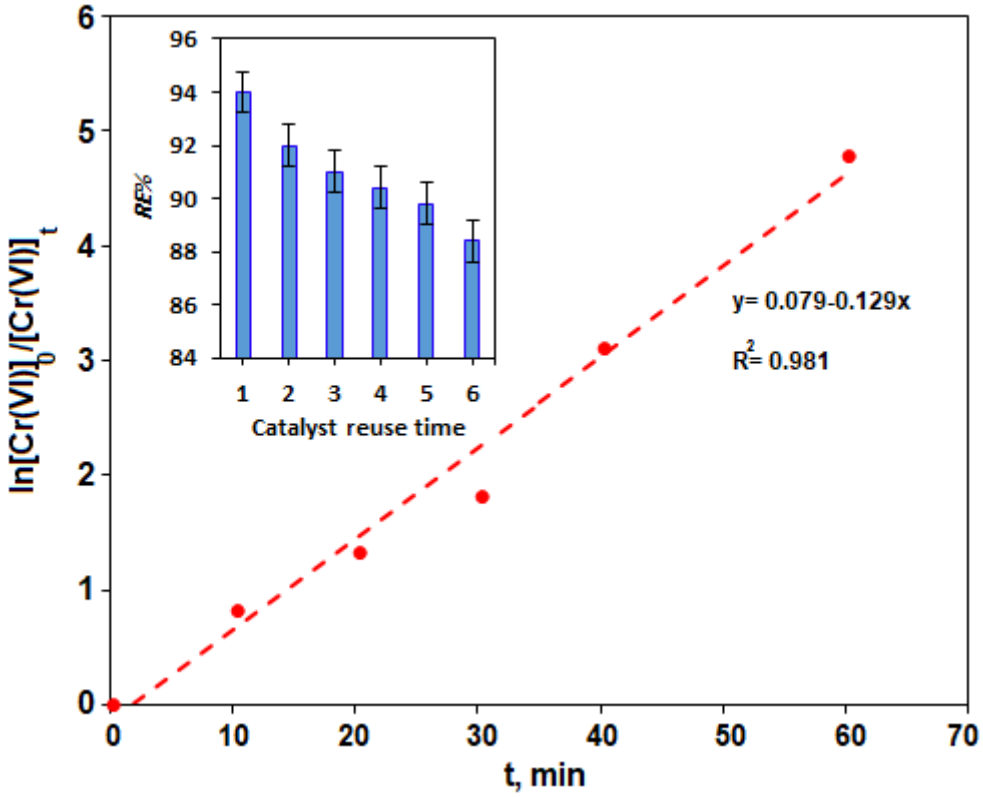
ln[Cr(VI)]0/[Cr(VI)]t
t, min
y= 0.079-0.129x
R2= 0.981
RE%
Catalyst reuse time

Fig. 8

Figures

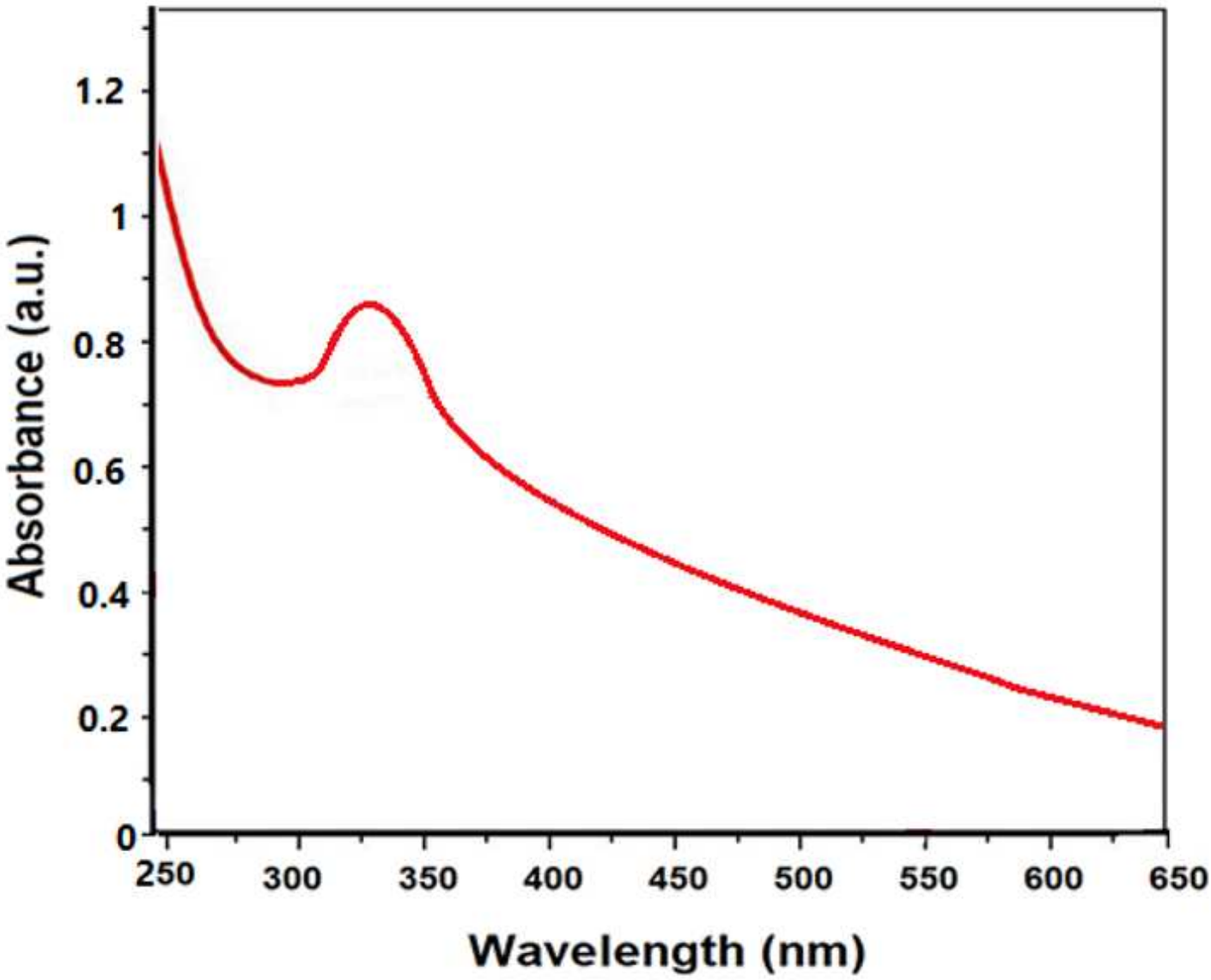

Figure 1

The UV-Vis spectrum of the biosynthesized CeO2-NPs

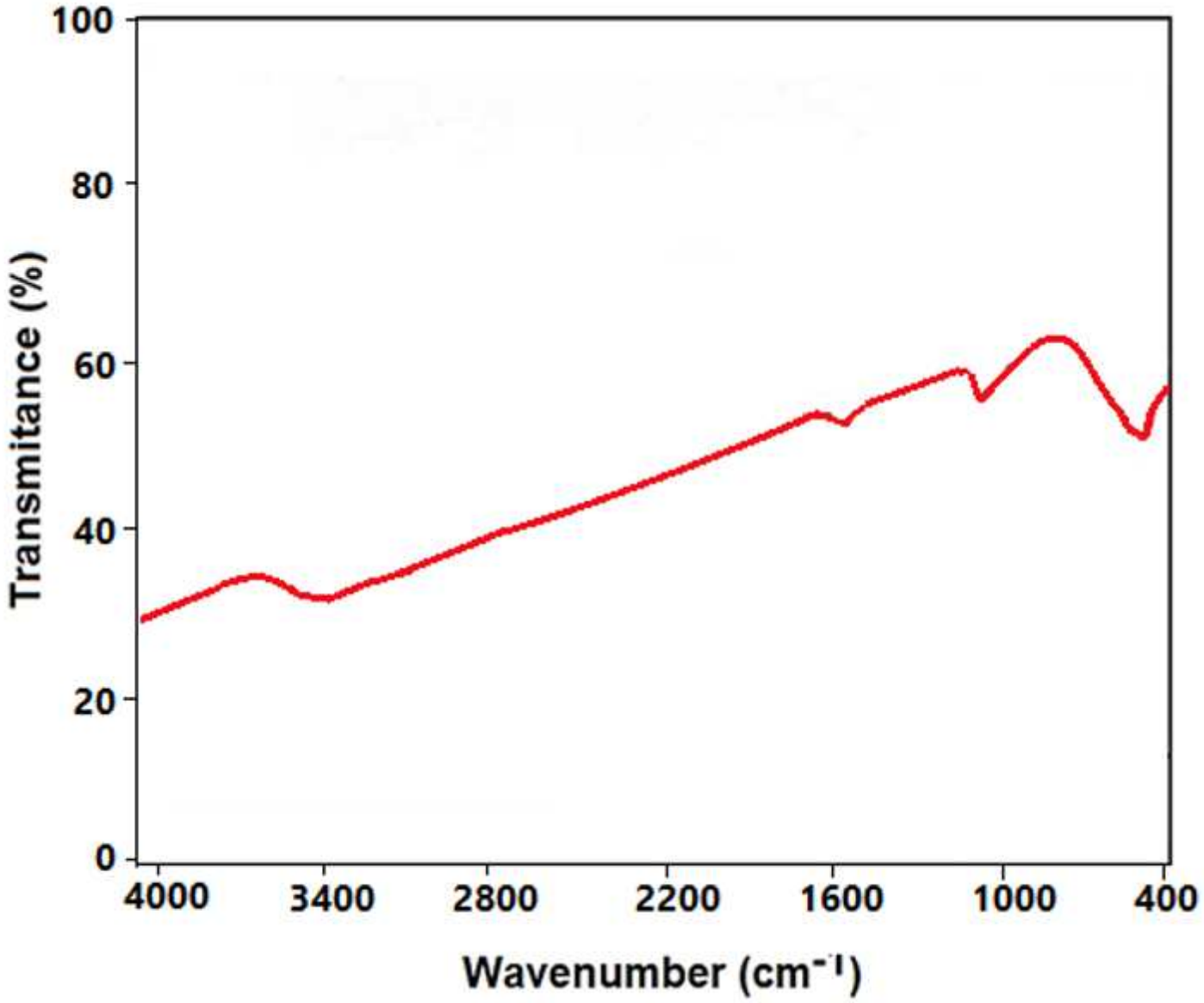

Figure 2

The FT-IR spectrum of the biosynthesized CeO2-NPs

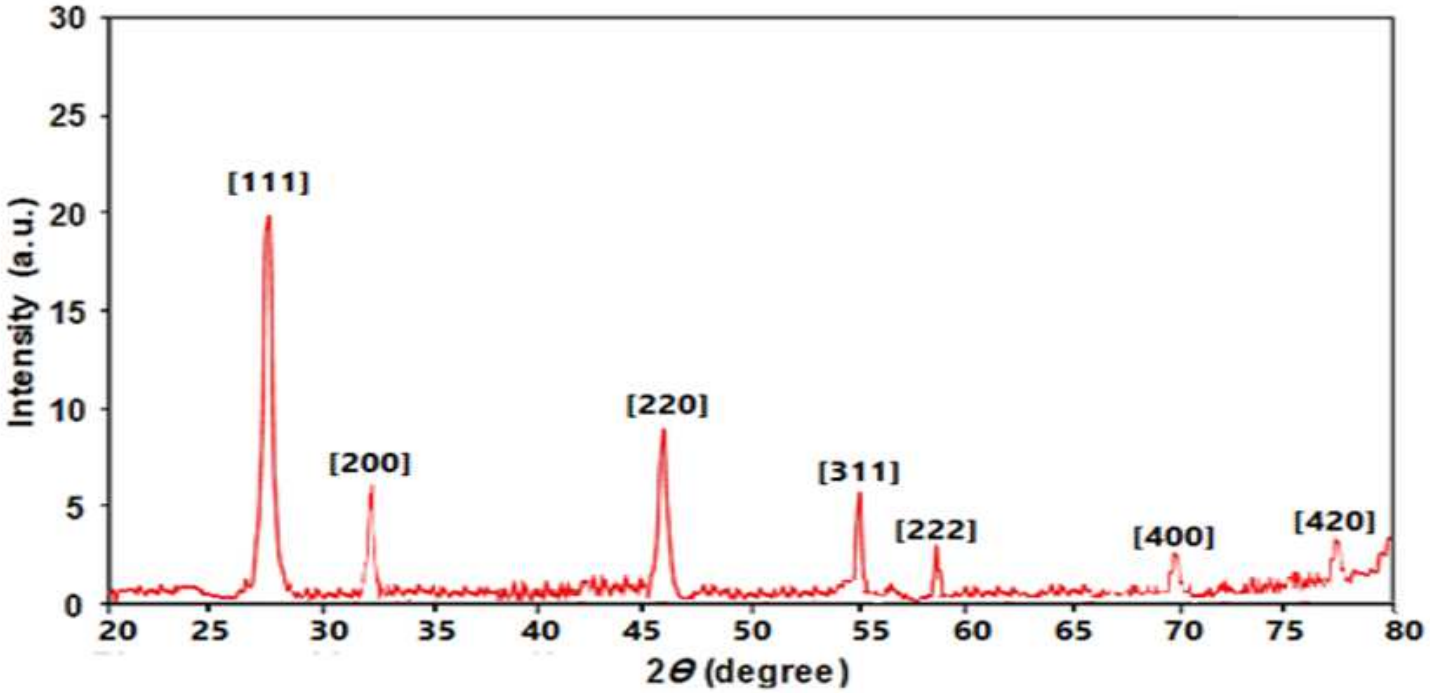

Figure 3

XRD patterns of the biosynthesized of CeO2-NPs

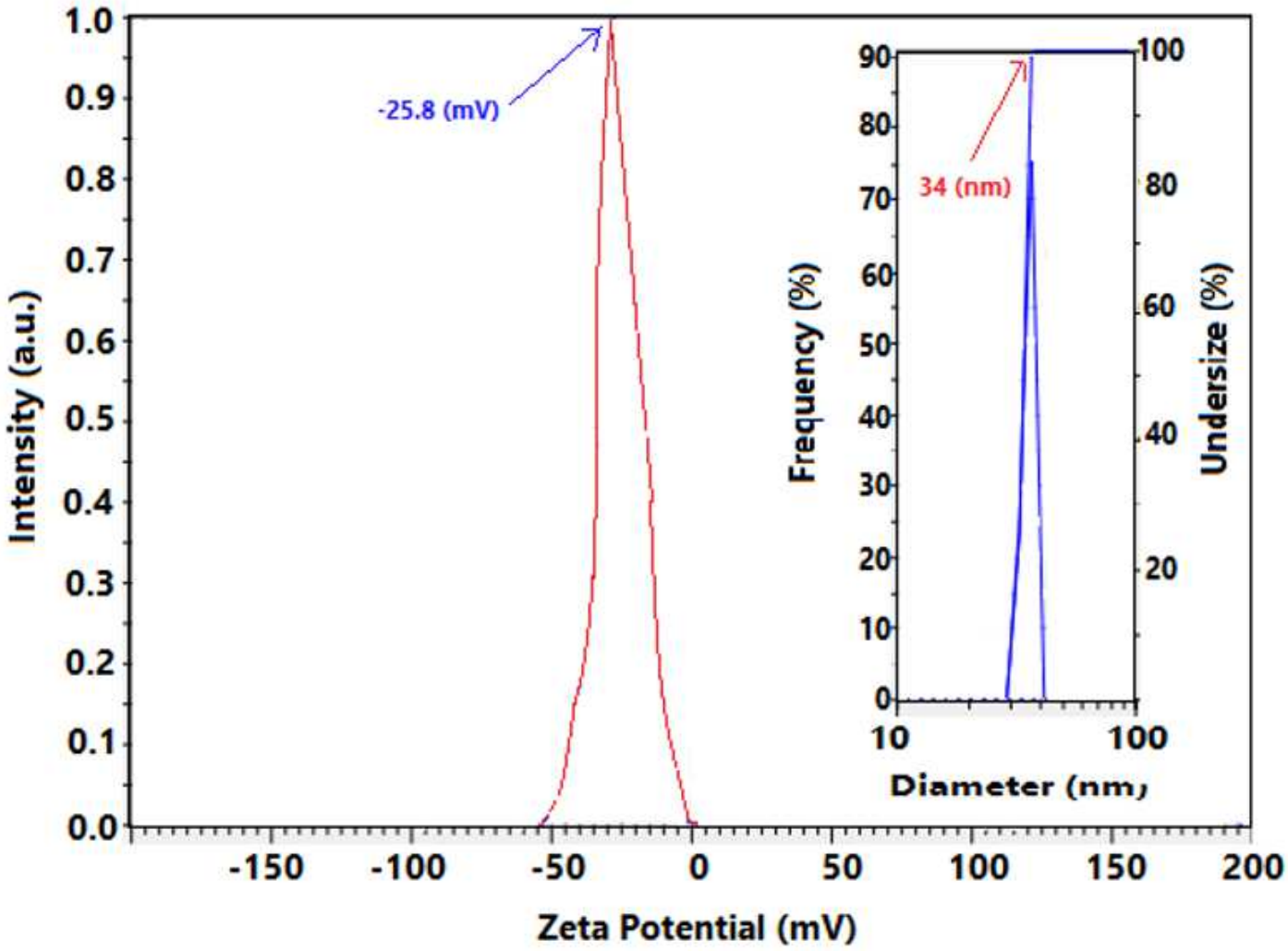

Figure 4

Zeta potential charge (ZPC) and the hydrodynamic particle size distribution (inset figure) of the biosynthesized CeO2-NPs

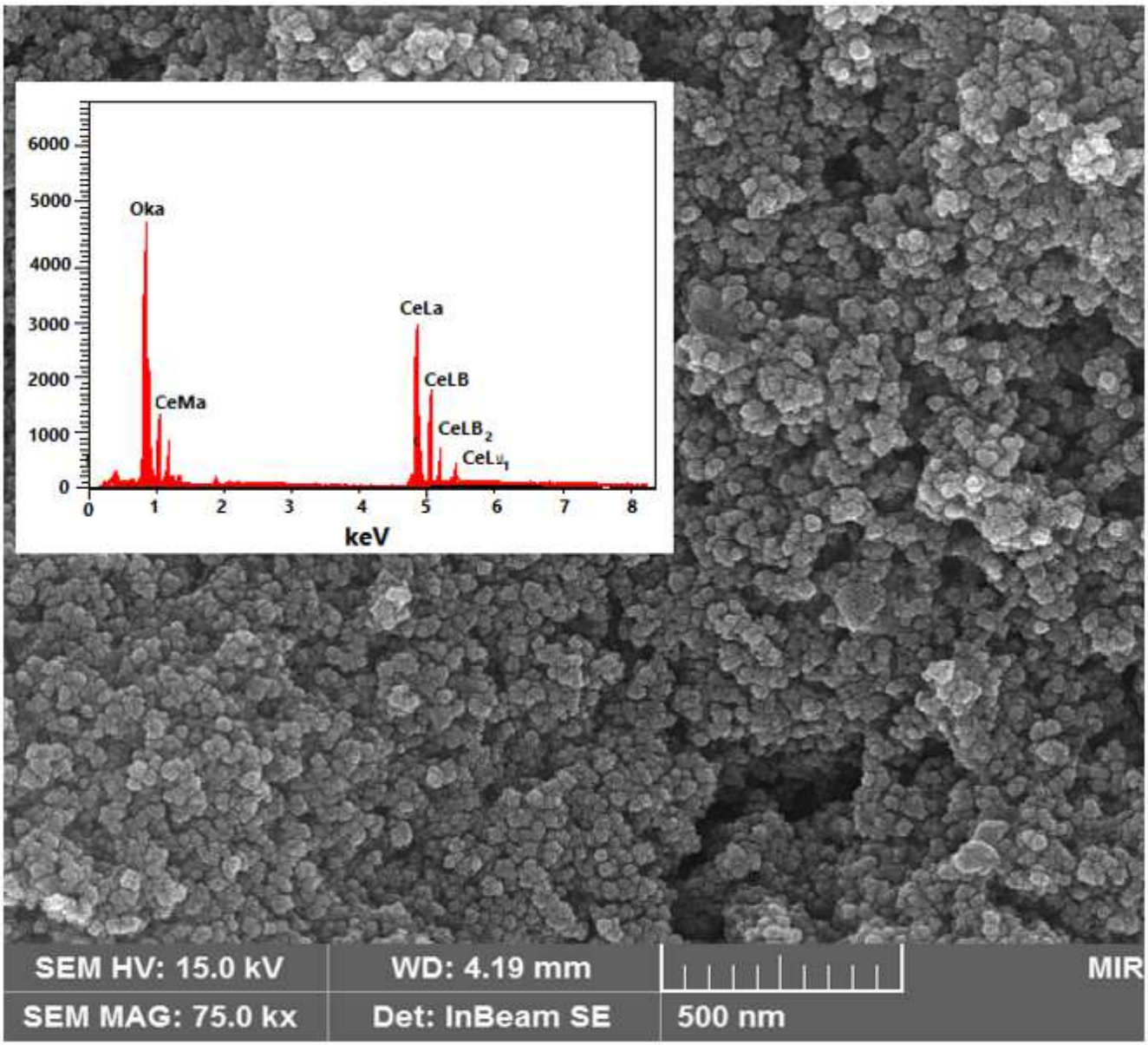

Figure 5

The FE-SEM image and EDX spectrum (inset figure) of biosynthesized of CeO2-NPs.

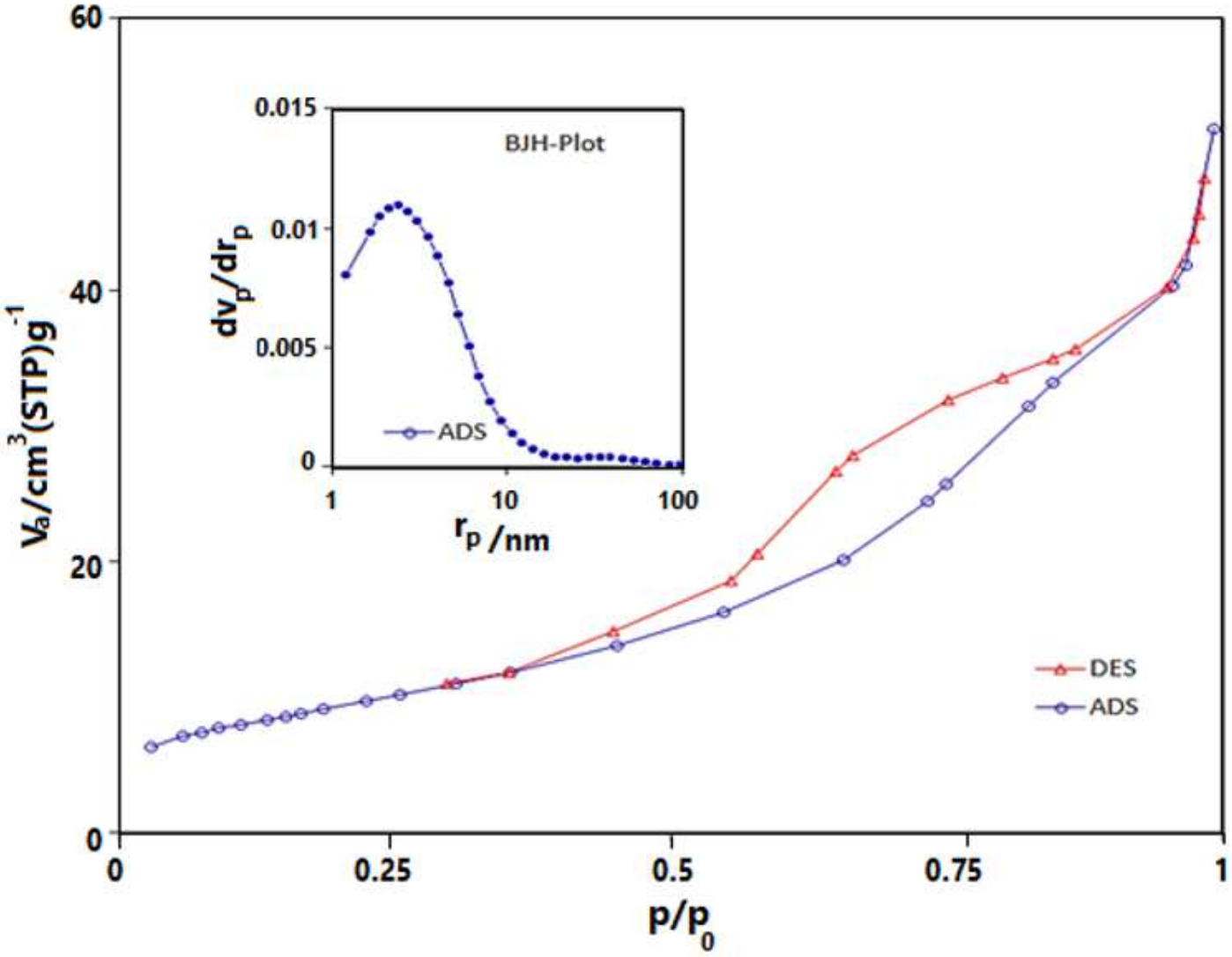

Figure 6

N2 adsorption-desorption isotherm of the biosynthesized CeO2-NPs. The inset figure is the pore radius distribution of CeO2-NPs

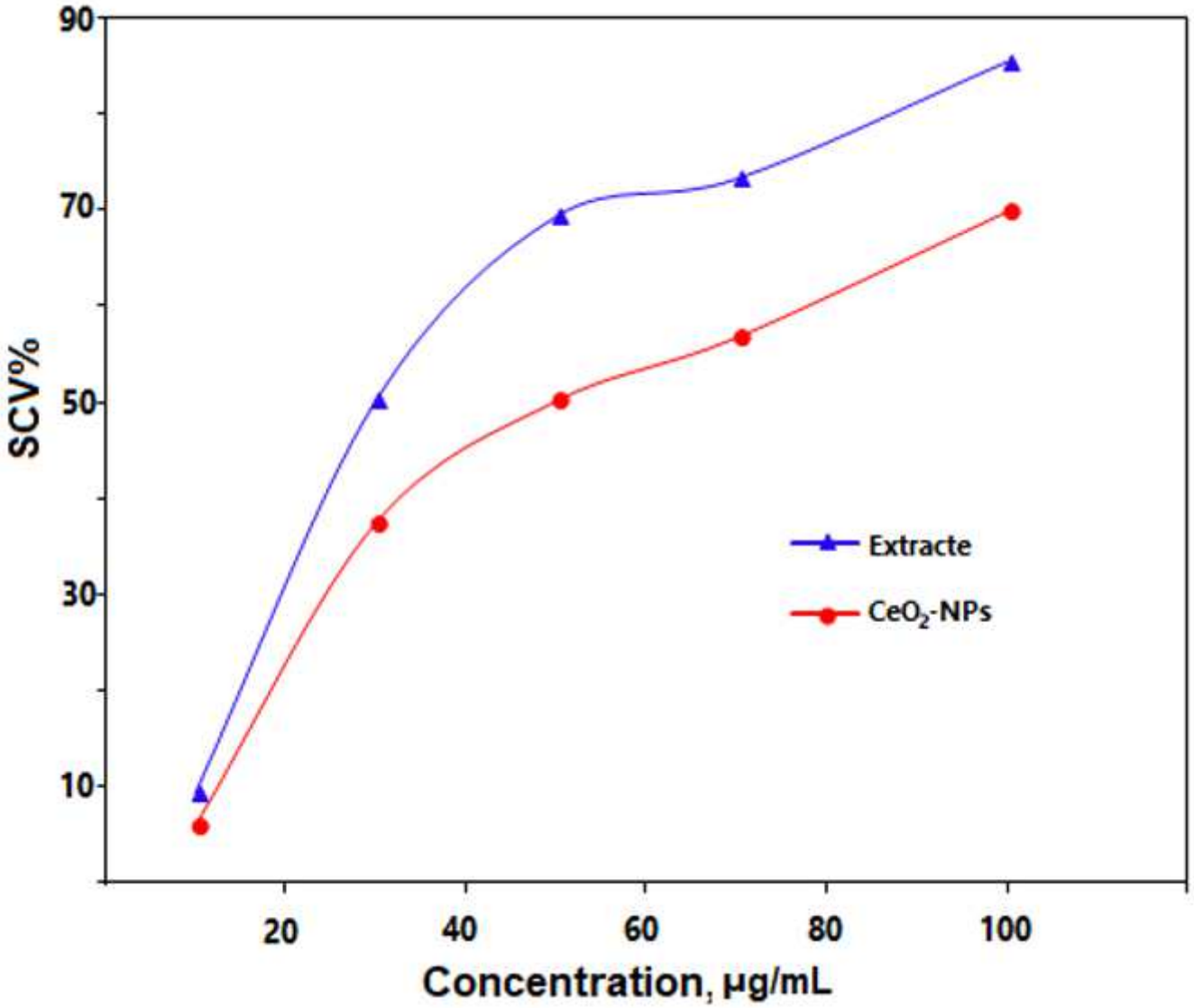

Figure 7

A comparison the antioxidant potential of the Pelargonium extract and biosynthesized CeO2-NPs

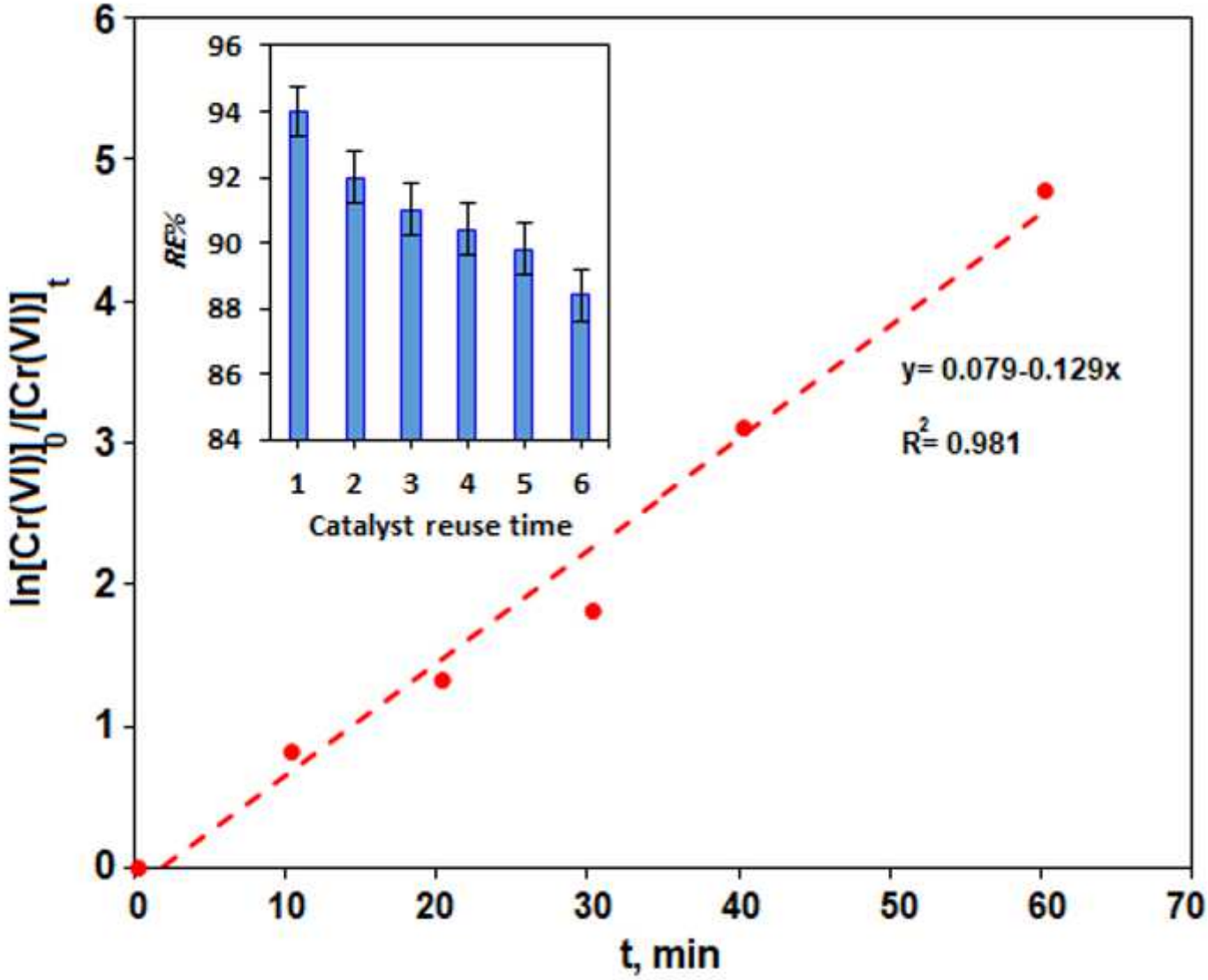

Figure 8

The kinetic plot in photocatalytic reduction of Cr(VI) ions under: [Cr(VI)]= 10 mg/L, [CeO2-NPs]= 200 mg/L, pH = 5.5 and t= 60 min. The inset figure is the reuse time results of biosynthesized CeO2-NPs catalyst